COMPUTATIONAL AND EXPERIMENTAL DEVELOPMENT OF NOVEL HIGH TEMPERATURE ALLOYS

M.J. Kramer, P.K. Ray and M. Akinc
Ames Laboratory and Department of Materials Science and Engineering,
Iowa State University, Ames, Iowa 50011

ABSTRACT

Building on our previous work of extending the Miedema (semi-empirical) model, we have started our initial screening of prospective alloys. Our approach is to closely couple the semi-empirical methodologies to more accurate *ab initio* methods to identify the best candidates for ternary alloying additions. The architectural framework for our material's design is a refractory base metal with a high temperature intermetallic which provides both high temperature creep strength and a source of oxidatively stable elements. Potential refractory base metals are groups IIIA, IVA and VA. For Fossil applications, Ni-Al appears to be the best choice to provide the source of oxidatively stable elements but this system requires a 'boost' in melting temperatures to be a viable candidate in the ultra-high temperature regime (> 1200°C). Some late transition metals and noble elements are known to increase the melting temperature of Ni-Al phases. Using a combination of our semi-empirical approach, *ab initio* calculations and experimental validation, we have demonstrated that Rh and Pd are the best candidates to boost stability of the NiAl phase while maintaining low solubility within many of the backbone refractory base metals. *Ab-initio* studies on the role of Rh and Pd on stability of NiAl, experimental studies on site preferences and a roadmap for our future work is presented with some preliminary oxidation studies to demonstrate the feasibility of this alloy design approach.

INTRODUCTION

Increases in operating temperatures of gas turbines are expected to result in increased Carnot efficiencies. An increase in operating temperatures entails with it an inherent loss in creep strength and significantly elevated oxidation rates. Additionally, the alloys in the gas turbines in power generation industries are exposed to coal combustion environment, resulting in exposure to steam, CO, SO_x, NO_x etc. Hence, the key challenge in high temperature alloy industry is the development of alloys that can function at higher and higher temperatures so that the balance between life-time and down-time stays positive [1].

Ni-based superalloys with a corresponding Ni-Al based coating is used for service temperatures in excess of 1000°C. Commercial overlay coatings are typically MCrAlY alloys, whereas diffusion coatings are based on β-NiAl. The choice of coating materials is dictated by their

ability to form strong bonding with the substrate, formation of an adherent slow-growing thermally grown oxide (TGO), and high temperature thermodynamic and microstructural stability [2]. Maximum temperature capability of current commercial coatings is limited to 1150°C. However, the objectives of FutureGen project require alloys that can function at about 1350°C. Hence, design of ultra high temperature alloys is a major task in DOE NETL's FutureGen gas turbine program. Such large increases in operating temperatures will require new materials and new engineering. An Edisonian approach to the discovery of new materials is tedious and we lack the numerical tools to efficiently predict new phases. A rapid means of 'sieving' through this phase space to identify the most promising combinations is necessary.

We attempt to tackle this problem by taking an integrated approach by combining the speed of semi-empirical calculations, with the accuracy of ab-initio studies and validate the computational approach with targeted experimental studies. In this paper, we use this integrated approach to study the role of transition metal additions to the B2 NiAl alloy. This study forms a small, but crucial section of our attempts at developing novel high temperature alloys for the coal combustion environments as well as other high temperature structural applications.

THEORY

The semi-empirical calculations were performed using an extended Miedema approach. According to this approach, the formation enthalpy is given as:

$$\Delta H = \phi_1 \Delta H_{AB}(c_A) + \phi_2 \Delta H_{BC}(c_B) + \phi_3 \Delta H_{CA}(c_C) \quad (1)$$

where c_A, c_B and c_C are atom fraction of species A, B and C in the AB, BC and CA binaries respectively and ϕ_1, ϕ_2 and ϕ_3 are weights assigned to each of the binaries. These weights are found by minimizing ΔH under the following set of constraints:

$$\begin{aligned} &\sum_{i=1}^{3} \phi_i = 1 \\ &\phi_1 c_A + \phi_3 (1 - c_C) = x_A \\ &\phi_2 c_B + \phi_1 (1 - c_A) = x_B \\ &\phi_3 c_C + \phi_2 (1 - c_B) = x_C \end{aligned} \quad (2)$$

Once the values of the weights and binary compositions have been determined, the formation enthalpy can be easily computed.

The formation enthalpies of the constituent binary systems are calculated using Miedema's semi-empirical model [3-9]. According to this model, the net enthalpy of mixing is given by the relation:

$$\Delta H_{tot} = \Delta H_{ch} + \Delta H_{el} + \Delta H_{st} \quad (3)$$

where ΔH_{ch}, ΔH_{el}, ΔH_{st} represent the chemical, elastic and structural contributions respectively. The chemical enthalpy may be evaluated as follows –

$$\Delta H_{ch} = c_A c_B \{ f_B^A \Delta H_{ic}^{AB} + f_A^B \Delta H_{ic}^{BA} \} \quad (4)$$

f_B^A represents the degree to which A is surrounded by B, and is given as:

$$f_B^A = c_B^s[1+\gamma(c_A^s c_B^s)^2] \quad (5)$$

where c_A^s represents the concentration of A at the surface and ΔH_{ic}^{AB} represents the interfacial enthalpy for A surrounded by B. The factor γ takes the values 8, 5 and 0 for intermetallics, metallic glasses and solid solutions respectively. The surface concentrations may be given as –

$$c_B^s = \frac{c_B V_B^{2/3}}{c_A V_A^{2/3} + c_B V_B^{2/3}} \quad (6)$$

The interfacial enthalpy is given by –

$$\Delta H_{ic}^{AB} = \frac{V_A^{2/3}}{(n_{ws}^{-1/3})_{av}}\{-P(\Delta\phi^*)^2 + Q(\Delta n_{ws}^{1/3})^2\} \quad (7)$$

The values of *P* and *Q* are dependent on the type of metals forming the alloy / intermetallic compound. Usually, the value of P is taken as 14.2 for metals with valency higher than 2, and 10.7 for metals with valency of 1 or 2. The *P/Q* ratio is maintained at 9.4 [3, 9]. Equation 7 has to be modified for alloys of a transition metal with a non-transition metal due to an additional enthalpy term, *R**, arising out of filling of Brillouin zones of a particular crystal structure. The modified relation may be expressed as –

$$\Delta H_{ic}^{AB} = \frac{V_A^{2/3}}{(n_{ws}^{-1/3})_{av}}\{-P(\Delta\phi^*)^2 + Q(\Delta n_{ws}^{1/3})^2 - R^*\} \quad (8)$$

The volume changes associated with charge correction effects may be given as [7] –

$$\Delta V_i = \frac{1.5 c_j^s V_i^{2/3}(\phi_i^* - \phi_j^*)}{2(n_{ws}^{-1/3})_{av}}(n_{ws,i}^{-1} - n_{ws.j}^{-1}) \quad (9)$$

$$V_i^* = V_i + \Delta V_i \quad (10)$$

Valence state of element determines the preferred crystal structure that it forms. Hence, during the process of alloying, if the elements are forced to form an alloy having a different crystal structure, an additional structural enthalpy term, needs to be added to the chemical enthalpy term. Miedema et al. proposed that the total structural enthalpy when an element "A" is dissolved in "B" is given by [10]:

$$H_{AinB}^{struct} = (Z_A - Z_B)\frac{\partial E^{struct}(B)}{\partial Z} + \left(E_B^{struct} - E_A^{struct}\right) \quad (11)$$

Once the structural contribution to the enthalpy is estimated, the formation enthalpy of an A-B binary would be given as:

$$\Delta H(A,B) = x_A x_B\left[\left(f_B^A H_{AinB}^{i/c} + f_A^B H_{BinA}^{i/c}\right) + \left(x_B H_{AinB}^{struct} + x_A H_{BinA}^{struct}\right)\right] \quad (12)$$

The first principles calculations carried out in the present work using the Vienna ab-initio simulation package (VASP) within the framework of the density functional theory (DFT). The calculation is conducted in a plane-wave basis, using the projector-augmented wave (PAW) method. The exchange and correlation items are described by the general gradient approximation (GGA). A 54-atom supercell was used for our calculations, and the substitution levels changed by substituting the ternary addition in Ni and Al sites.

EXPERIMENTAL DETAILS

Alloys with nominal compositions $Ni_{50-x}Al_{50}M_x$ and $Ni_{50}Al_{50-x}M_x$ with x = 0, 3, 6, 9 and M = Pd, Rh, Zr and Hf were synthesized from pure metals by arc-melting. The alloys were arc-melted four times to ensure homogeneity. This was followed by annealing in Argon atmosphere for 6 hours at 1300^{o}C. The alloys were then characterized using x-ray diffraction and scanning electron microscopy. Microstructures of the alloys were studied using a JEOL 5910LV scanning electron microscope at an accelerating voltage of 20kV. Phase analyses of the alloys were carried out using a Philips PANalytical x-ray diffractometer using the Cu Kα radiation with a step size of 0.008 degrees. The x-ray data was then Rietveld refined using GSAS [11] to determine the change in lattice parameters. Alloys containing Hf and Zr exhibited a eutectic microstructure and the alloys reacted easily with Ta crucible during the heat treatment process and were not considered for further single crystal studies.

Single crystals from the heat treated samples were mounted on the tip of a glass fiber. Room temperature intensity data were collected on a Bruker Smart Apex CCD diffractometer with Mo K_α radiation (λ = 0.71073 Å) and a detector-to-crystal distance of 5.990 cm. Data were collected over a full sphere of reciprocal space by taking three sets of 606 frames with 0.3° scans in ω with an exposure time of 10 seconds per frame. The 2θ range extended from 4° to 57°. The *SMART* [12] software was used for data acquisition. Intensities were extracted and then corrected for Lorentz and polarization effects by the *SAINT* [12*]* program. Empirical absorption corrections were accomplished with the program *SADABS* [12], which is based on modeling a transmission surface by spherical harmonics employing equivalent reflections with $I > 3\sigma(I)$. Structure solutions and refinements were performed with the *SHELXTL* [12] package of crystallographic programs.

In addition to the structural characterization, flowing air studies were also carried out to assess the effect of the ternary additions on oxide scale formation in these alloys. The flowing air studies were carried out at 1150^{o}C by exposing the alloys to flowing air inside a tube furnace for 25 hours.

RESULTS AND DISCUSSION

The basic objective of ternary additions is to enhance the melting temperature of the B2 NiAl. The formation enthalpy can be regarded as a criterion for thermodynamic stability, and in general, a higher formation enthalpy corresponds to an increased stability. The extended Miedema approach was used to compute the formation enthalpies of a large number of alloy systems, and the alloying additions that result in significantly more negative formation enthalpies were screened out. Amongst these additions, the elements that stabilized the liquid phase or formed a porous non-volatile oxide were discarded, and the *ab-initio* studies were carried out with the remaining ternary additions. Based on the *ab-initio* calculations the prospective systems were selected for experimental studies.

Based on the calculations, Pd, Rh, Zr and Hf were found to lower the formation enthalpies when added to NiAl. Hence the experimental studies were carried out using these alloys. Figures 1a-d show the typical microstructures of $Ni_{50-x}Al_{50}M_x$ alloys (M = Pd, Rh, Zr and Hf for x = 9). It can be seen that Hf and Zr modified NiAl exhibit a two phase alloy, with a eutectic microstructure, whereas Pd and Rh modified alloys show a single-phase microstructure. Since the presence of an eutectic will lower the overall melting temperature for the alloy, further studies were focused only on Pd and Rh containing alloys.

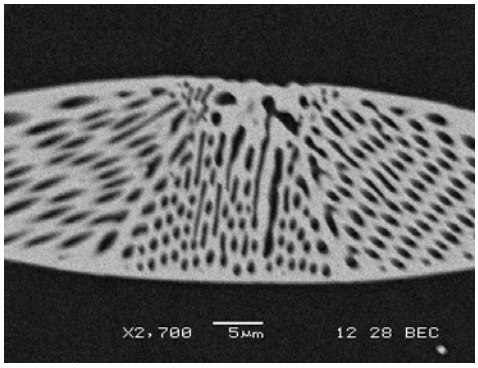

a): Ni-Al-Hf alloys

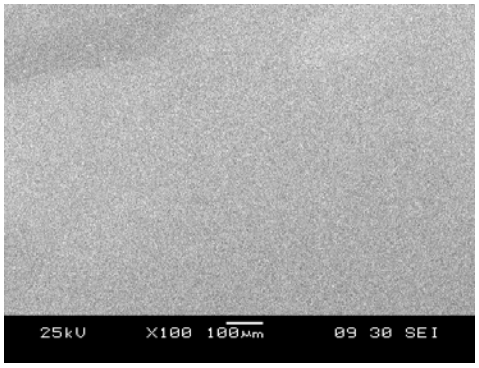

b): Ni-Al-Pd alloys

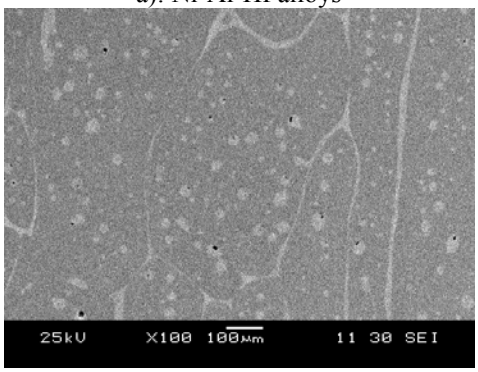

c): Ni-Al-Zr

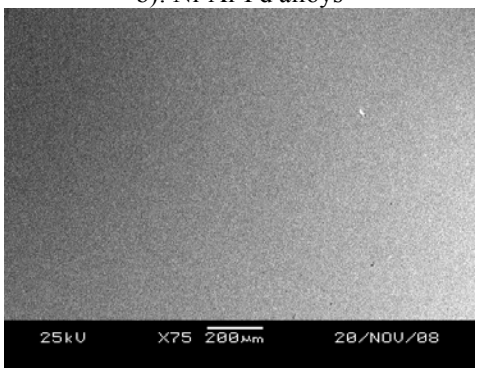

d): Ni-Al-Rh

Figure 1. Micrstructure of arc-melted, annealed ternary alloys: Ni-Al-M where M is a) Hf, b) Pd, c) Zr, and d) Rh

Figure 2shows the result of *ab-initio* calculations in the two key systems, namely Ni-Al-Pd and Ni-Al-Rh. It can be seen that in both cases, substituting the transition metal in Ni site results in a lower formation enthalpy as opposed to substitution in the Al site, indicating a marked preference for these transition metals to occupy the Ni site. These theoretical calculations were then verified using a combination of single crystal as well as powder x-ray diffraction experiments. Single crystal x-ray studies confirmed that the Pd and Rh prefer the Ni sites rather than the Al sites. The lattice parameter variation with increased substitution levels of Rh and Pd were studied using powder x-ray diffraction. Lattice parameters increased monotonically with increased amounts of ternary additions. Figure 3 shows the variation of lattice parameters in case of the Pd modified B2 NiAl. In addition to the experimentally determined lattice parameters,

theoretically calculated lattice parameters have been plotted as well. It can be seen that there is a fairly good agreement between theory and experiments.

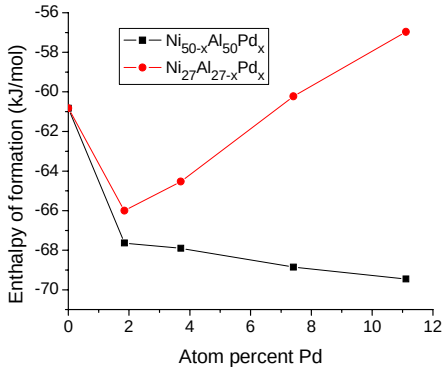

Figure 2a: Variation in formation enthalpy with Pd addition in Ni and Al sites

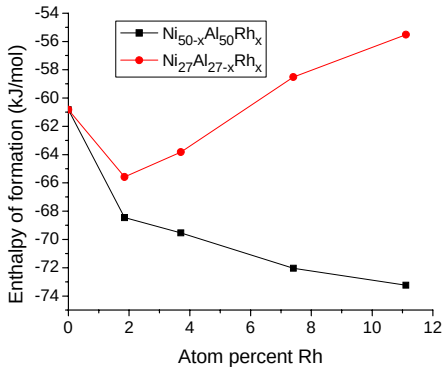

Figure 2b: Variation in formation enthalpy with Rh addition in Ni and Al sites

Using the calculated formation enthalpies, the melting temperatures were estimated using the Rose-Ferrante expression:

$$T_m = 0.092\frac{\Delta E}{k_B}$$

( ).

In this relation the ΔE has been calculated as follows:

$$\Delta E = \sum E_i - \Delta H^{form}$$

,

where ΔH^{form} is the enthalpy of formation and E_i is the cohesive energy of the 'ith' element. The calculated results have been shown in Figure 4. It should be stressed that the Rose-Ferrante relation was developed for pure metals; however, it has been shown to hold within reasonable limits for metallic alloys as well. In our work, we have used this relation to obtain an estimate of the melting temperatures of the ternary element modified B2 NiAl rather than absolute values. High temperature differential thermal analysis studies are in progress to check the validity of these calculations.

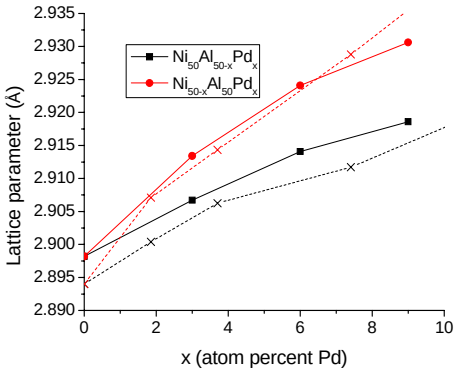

Figure 3. Lattice parameter variation with increased Pd content. The experimental values are indicated using solid lines and the theoretical values are indicated using dotted lines.

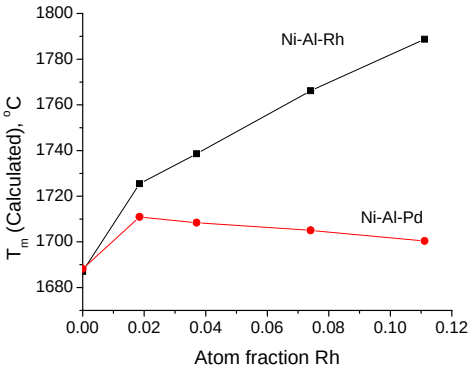

Figure 4: Variation of melting temperature with alloying additions

Comment [M1]: I would use either atom fraction or atom % on both figures' horizontal axes

The representative oxidized microstructures are shown in Figure 5. Figure 5a shows the oxidized microstructure of un-doped NiAl. The microstructures with 9 atom percent Pd and Rh additions are shown in 5b and 5c respectively. It can be seen that addition of Pd and Rh resulted in formation of a thinner continuous scale and hence has a positive influence on oxidation behavior.

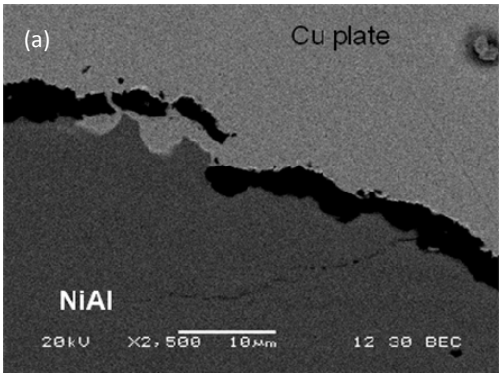

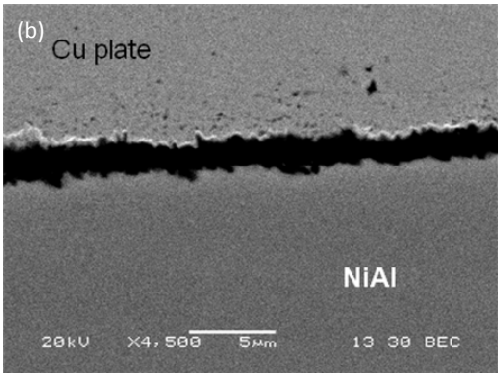

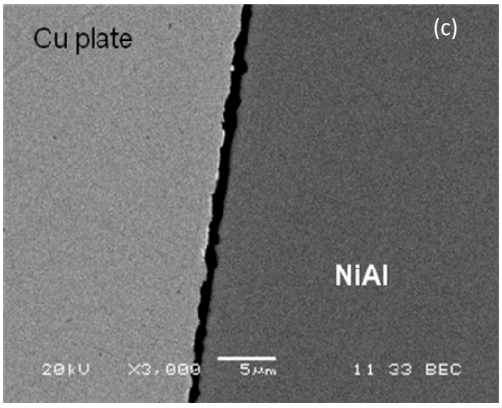

Figure 5: Microstructures of alloys oxidized in flowing air at 1150°C for 25 hours.
(a) NiAl without any alloying additions
(b) $Ni_{41}Al_{50}Rh_9$
(c) $Ni_{41}Al_{50}Pd_9$

CONCLUSIONS

In this study, we have demonstrated an approach that combines semi-empirical, *ab-initio* calculations with experimental work. This approach was used to down-select potential ternary additions to B2-NiAl, followed by more detailed studies on the effect of these additions on the stability of the B2 NiAl phase. It is expected that Pd and Rh additions will help improve the high temperature stability of NiAl, with Rh being more effective than Pd. Rh and Pd have also resulted in improved oxidation behavior. Future studies will focus on phase assemblage of a Mo-based solid solution with the substituted NiAl as the reinforcing oxidation resistant phase.

REFERENCES

[1] J. R. Nicholls, MRS Bulletin 28 (2003) 659-670.
[2] S. W. Wang, Oxidation of Metals 15 (1981) 1573.
[3] F. R. d. Boer, R. Boom, W. C. M. Mattens, A. R. Miedema, A. K. Niessen, Cohesion in metals: Transition Metal Alloys North Holland, Amsterdam, 1988.
[4] A. R. Miedema, A. K. Niessen, Calphad 7 (1983) 27-36.
[5] A. K. Niessen, F. R. de Boer, R. Boom, P. F. de Chatel, W. C. M. Mattens, A. R. Miedema, Calphad 7 (1983) 51-70.
[6] A. R. Miedema, Journal of the Less Common Metals 46 (1976) 67-83.
[7] A. R. Miedema, A. K. Niessen, Physica 114B (1982) 367-374.
[8] A. R. Miedema, Physica B 182 (1992) 1-17.
[9] A. R. Miedema, P. F. de Chatel, F. R. de Boer, Physica B+C 100 (1980) 1-28.
[10] H. Bakker, Enthalpies in Alloys: Miedema's semi-empirical model, Trans Tech Publications, Switzerland, 1998.
[11] B. H. Toby, Journal of Applied Crystallography 34 (2001) 210-213.
[12] XRD Single Crystal Software, in: Bruker Analytical X-ray Systems, Madison, 2002.